Optimization of monopile offshore wind structures

A. THIRY, F. BAIR, L. BULDGEN, G. RABONI & P. RIGO
University of Liège, ANAST, Liège, Belgium

ABSTRACT: As industrialization is essential for large-scale offshore wind deployment, a computerized methodology to optimize the scantling of monopile steel structures has been developed using a genetic algorithm. The objective functions of this tool are minimization of the structure weight and production costs. The constraints implemented are mainly related to structural stability under extreme loads, resonance check of the wind turbine support and fatigue strength at welded connections between shells and stiffeners. This optimization should be invoked at the preliminary stage of the offshore project in order to assess the impacts of the structure design on the fabrication and installation costs.

1 INTRODUCTION

Since the very beginning of the century, wind market has started to move offshore. Indeed oceans locations offer a higher wind quality and the visual impact of wind farms is significantly reduced. Offshore wind power is now expected to represent an important share of the future power supply both in Europe and worldwide, reducing dependency of industrial countries toward fossil fuels.

The main driver behind the methodology exposed in this paper is the improvement of classical steel solutions dedicated to monopile structures used in offshore wind industry (Fig. 1). A structural optimization tool has thus been implemented to investigate the gains in terms of weight and production costs generated by the use of high tensile steel for shells, as well as longitudinal and circumferential stiffeners.

Figure 1. Steel monopile offshore wind turbines.

2 GENERAL SCHEME OF THE OPTIMIZATION TOOL

The flowchart of the optimization tool described in this paper is presented on Figure 2. The input data implemented by the designer of the project are the starting point of the computation. They are related to the environment at the offshore location, the characteristics of the wind turbine and the scantling of the support structure (without any consideration about the underground part of the monopile).

The set of selected design variables and input data are then used as a basis to assess the objective function (weight or production cost) and the constraints (structural integrity) of the monopile structure.

A genetic algorithm finally combines these two elements – objective function and structural integrity – over a certain number of iterations in order to find the optimum scantling of the support structure placed in the given external conditions.

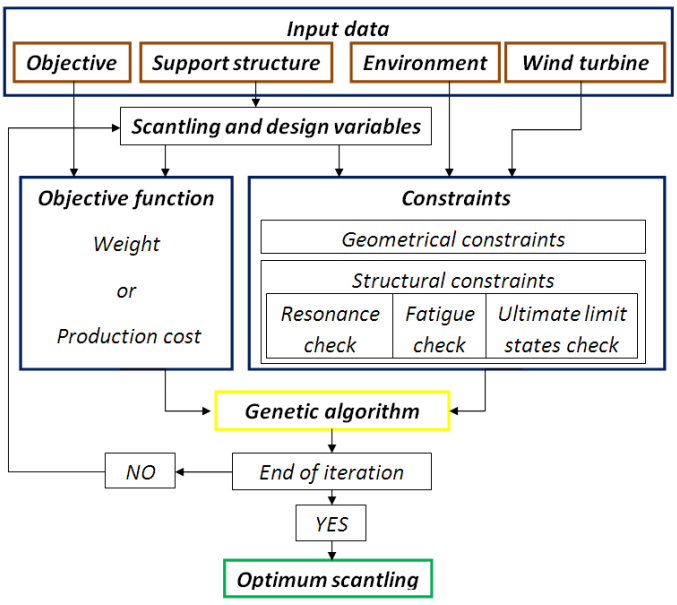

Figure 2. General scheme of the optimization algorithm.

3 INPUT DATA

3.1 *Environment*

Environmental data summarizes the characteristics of the site, data related to fatigue analysis and load cases considered for the ultimate limit state analysis.

Firstly, site data contains the values for water depth d, the power law exponent α characterizing the vertical distribution of wind speeds over the tower height, the densities of the air ρ_a and of the sea water ρ_w.

Secondly, for fatigue concern a distinction is made between waves and wind actions. On one hand, waves participation is presented under the form of a list of sea states (or scatter diagram), each one being characterized by a significant wave height H_S, a mean zero up-crossing period T_Z and a percentage of occurrence of the sea state P_{SS}. On the other hand, spectrums of punctual tower top loads are used to describe fluctuating wind loadings on the structure.

Finally, data related to ultimate limit states are listed under the form of a series of environmental situations and their associated wind and waves conditions: average wind speed at hub height V_{hub}, water level elevation Δd compared to the mean still water level MSL (elevation due to tide or storm for example), wave height H_w and period T_w and a set of punctual tower top loads.

3.2 *Support structure*

The monopile offshore wind tower considered in the study is an assembly of several conical or cylindrical tubular segments. The segments themselves are made of shell rings linked together with butt welds. Each shell ring is characterized by a shell thickness, upper and lower diameters, a height, a steel grade and a category of detail for the butt weld.

Four framing systems are envisaged for the scantling of shells belonging to the same tower segment: unstiffened, longitudinally stiffened, ring stiffened or orthogonally stiffened shells.

3.3 *Wind turbine*

Some general data of the wind turbine are taken into account for this preliminary design of the monopile structure: the hub height H_{hub}, the number of blades n, the rotor diameter d_{rotor}, the weight of the rotor-nacelle assembly m_{Top}, the technical design lifetime of the turbine and its range of rotational speed.

The interface of the optimization tool is presented on Figure 3.

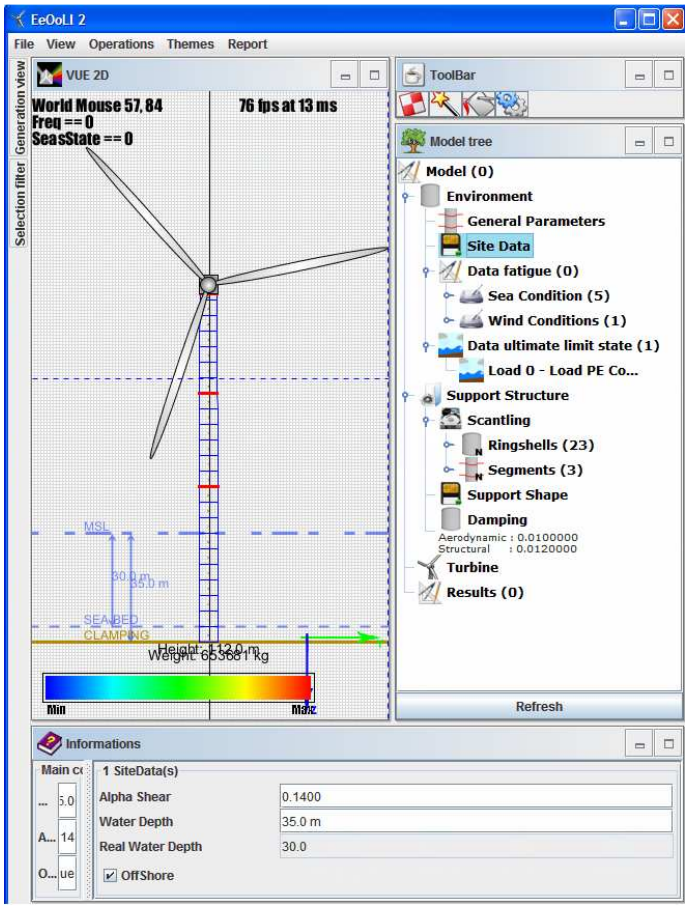

Figure 3. Screen shot of the optimization tool.

4 ASSESSEMENT OF CONSTRAINTS

4.1 *Generals*

The constraints implemented in the optimization process are typically divided in two categories: geometrical and structural constraints.

The first type of constraints refers to geometrical requirements such as equality of shell rings diameters in one segment or decrease of shell thicknesses and diameters while progressing to the top of the monopile structure.

The second type represents structural constraints related to the verification of the structural integrity of the offshore wind turbine towards fatigue, ultimate limit states and resonance phenomena. The verification of those constraints requires the use of either quasi-static or dynamic analysis of the structure.

4.2 *Building the 2D dynamic model*

In order to perform dynamic analyses, a simple 2D dynamic model made of concentrated masses connected together with a translational spring is built on the base of the scantling (Fig. 4). Nodes are located at the intersection between shell rings and are characterized by two degrees of freedom: one horizontal translation x_i and one in-plane rotation θ_i (vertical translations are not taken into account as they are supposed negligible compared to horizontal transla-

tions). The model is perfectly clamped at a distance from the sea bed level equal to the height of the first shell ring. This assumption allows the designer to take into account the length required for the complete soil restraint to develop around the monopile.

The aerodynamic damping generated by the rotor is modeled with a single dashpot connected to the tower top degree of freedom in translation and the structural damping is expressed as a combination of the generalized matrixes of masses [M*] and rigidity [K*] (Rayleigh damping).

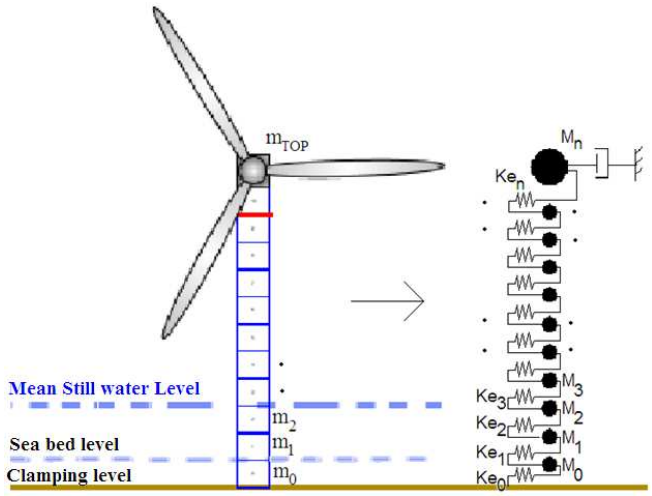

Figure 4. The 2D dynamic model of the offshore wind turbine studied in the optimization process.

The value and the distribution of masses of the wind turbine are not supposed to change. Thus, cases where the offshore structure is covered with a layer of ice or marine growth are excluded from the dynamic analysis.

Basically, the simplicity of the chosen dynamic model is justified by two considerations. On one hand, the optimization process requires a great number of iterations that should not take too much computation time. And, on the other hand, loss of accuracy in the results is not a major problem as the methodology is dedicated to early stage design.

4.3 *Resonance of the support structure*

Excitations are likely to occur at frequencies that are close to the natural frequencies of the offshore wind turbine, leading to resonance phenomena. Natural frequencies and corresponding modes of the support structure are defined respectively from the generalized eigen values λ and eigen vectors $\vec{V}$ of the matrixes of masses [M] and rigidity [K]. The Campbell diagram related to the excitation frequencies for the rotor motion (1n) and the blades passing (3n for a 3-bladed wind turbine) can then be used to check if resonance of the support structure is avoided within the rotational speed range of the wind turbine (Fig. 5).

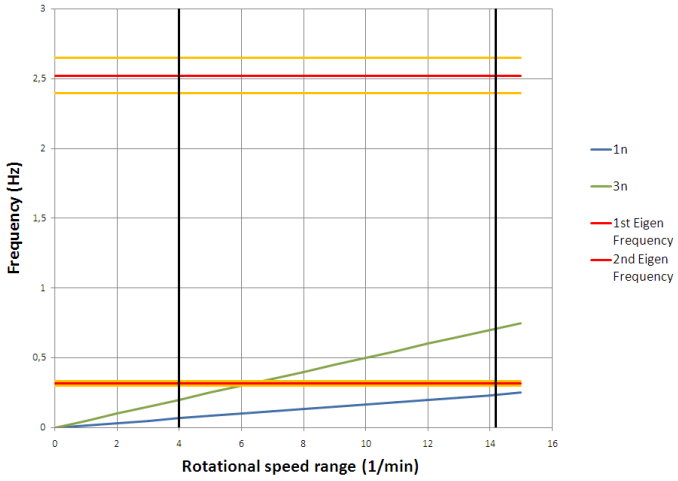

Figure 5. Campbell diagram for a 3-bladed offshore wind turbine.

4.4 *Fatigue check*

4.4.1 *Generals*

Fatigue strength is verified at each structural detail of the support structures (butt welds, ring-stiffener connections, etc.) thanks to the Miner rule (chech that cumulative fatigue damage $D_{fat} < 1$).

In addition, the procedure developed for fatigue analysis assumes that wind and waves effects are completely uncoupled. Hence, the total cumulative fatigue damage D_{fat} results from the addition of the fatigue damages due to wind actions $D_{fat,wind}$ and waves actions $D_{fat,wave}$.

Concerning the characteristics of the wind tower, structural members are supposed to be continuous and steel is considered as an isotropic and homogeneous material.

4.4.2 *Fatigue due to waves actions*

Over its life, the offshore wind turbine will experience series of sea states, each one generating cyclic loadings and being responsible for a certain percentage of the total cumulative fatigue damage due to waves $D_{fat,wave}$ in the structural components. Thus, for each sea state listed in the scatter diagram, the equations governing the dynamic of the structure and the stress range histogram at the nodes are solved using stochastic dynamic theory in the frequency domain.

In the first step of the computation, a fully developed sea at infinite fetch is assumed and the Pierson-Moskowitz wave spectrum PSD_H (equation 1) is generated at each frequency step for the concerned sea state.

$$\boldsymbol{PSD_H(f) = \frac{H_S^2}{4\pi T_z^4 f^5} e^{-\frac{1}{\pi}(fT_z)^{-4}}} \quad (1)$$

where H_S = significant wave height of the sea state; T_Z = mean zero-up crossing period; f = frequency.

Secondly, the value of the power spectral density of the water particles acceleration $PSD_{aw,i}$ is deduced from the Pierson-Moskowitz spectrum PSD_H according to equation 2.

$$PSD_{aw,i}(f) = PSD_H(f)\left(\frac{1}{2}.\frac{(2\pi f)^2 cos\,h\left(k_{wave}(z_i^*)\right)}{sin\,h(k_{wave}d)}\right)^2 \quad (2)$$

where k_{wave} = wave number; z_i^* = vertical position of the node i from sea bed level; d = water depth; i = numbering of the node in the dynamic model.

Once the water particles acceleration spectrum $PSD_{aw,i}$ is established for each underwater nodes of the model, the distribution of hydrodynamic inertia loads spectrum is computed in the matrix $[PSD_{Fwave}]$. Each element $PSD_{Fwave,i,j}$ of this matrix results from the Morison formulation and the coupling between nodal forces inherent to the stochastic theory (equation 3).

$$PSD_{Fwave,i,j} = \begin{cases} A_i\sqrt{PSD_{aw,i}} \;.\; A_j\sqrt{PSD_{aw,j}} & \text{for } i,j \le n_{uw} \\ 0 & \text{for } i,j > n_{uw} \end{cases} \quad (3)$$

where n_{uw} = number of shell rings located below the mean still water level; A = parameter allowing calculation of wave loads and distribution of these loads on the nodes of the dynamic model (see equation 4).

$$A_i = C_m \rho_w \left(\frac{\pi D_i^2}{4}\right) L_{F,i} \quad (4)$$

where C_m = hydrodynamic inertia coefficient (taken equal to 2); ρ_w = sea water density; D_i = diameter of the structure at node i; $L_{F,i}$ = length of the part of structure submitted to the waves load above and below the node i.

Note that the hydrodynamic drag term is not taken into account in the analysis of wave induced fatigue. This is due to the fact that sea conditions considered for the fatigue analyses are less severe than in extreme waves conditions, making the hydrodynamic inertia load predominant in the Morison formulation.

The systems of equations are solved in the modal basis to get the power spectral densities of bending moments $PSD_{M,wave}$ in the structure at each frequency step. Power spectral densities of normal stresses $PSD_{\sigma,wave,i}$ in the structural details are then deduced using simple beam theory (see example on Figure 6).

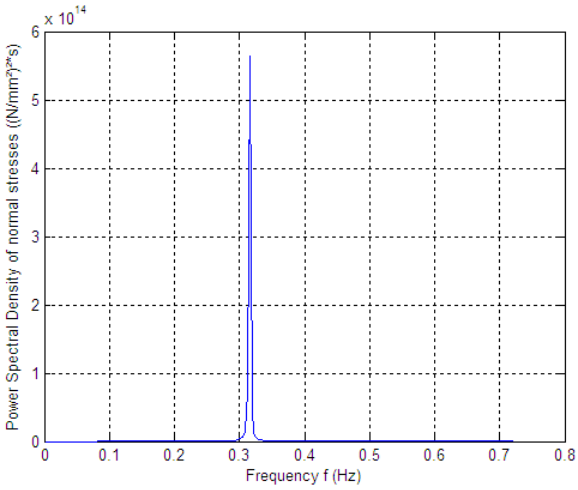

Figure 6. Power spectral density of normal stresses at the clamping point of a structure when H_S=0.25m and T_Z=4s.

In the next step of the computation, the Rayleigh counting method is invoked to assess the number of fatigue cycles n_{wa} and their associated stress range $S_{wa,k}$ characterizing the sea state (equation 5).

$$n_{wa}(S_{wa,k}) = T_d\sqrt{\frac{m_2}{m_0}}\left(P_{Rayeigh}(S_{wa,k+1}) - P_{Rayeigh}(S_{wa,k})\right) \quad (5)$$

where T_d = duration of the concerned sea state; m_0 = variance of the power spectral density of normal stresses $PDS_{\sigma,wave,i}$ at node i; m_2 = third spectral moment of the power spectral density of normal stresses $PDS_{\sigma,wave,i}$; $P_{Rayleigh}$ = probability of occurrence of the stress range $S_{wa,k}$.

Figure 7 shows the normal stress range histogram (n_{wa},$S_{wa,k}$) obtained from the power spectral density of normal stresses at the clamping point presented on Figure 6.

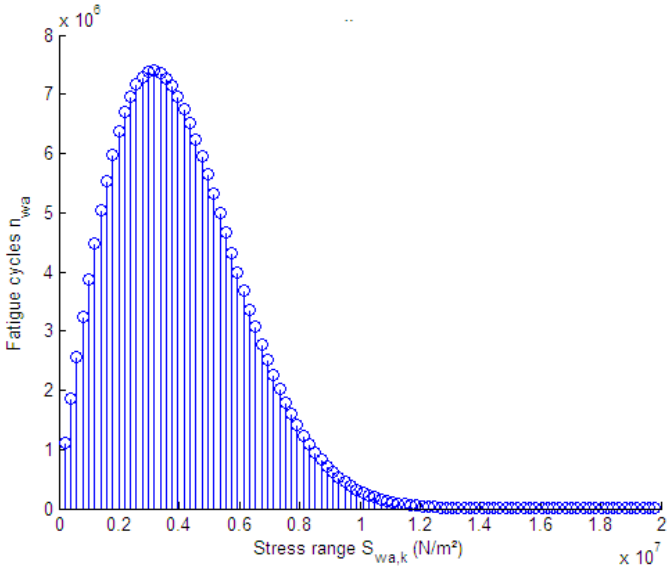

Figure 7. Normal stress range histogram of normal stresses at the clamping point of an offshore wind turbine.

At the end, the normal stress range histograms associated to each sea state are summed and conventional S-N curves based on the detail category are used to assess the cumulative fatigue damage due to waves $D_{Fat,wave}$.

4.4.3 *Fatigue due to wind action*

For the preliminary design procedure developed in this study, wind loads coming from the rotor-nacelle assembly are completely uncoupled from the dynamic of the support structure. Physically, this approach means that the "transfer" between the 3D wind speeds field and the tower top loads is performed considering that the turbine is connected to an infinitely rigid support. As a result, the value of the cumulative fatigue damage due to wind $D_{Fat,wind}$ is only based on the variations of tower top loads and their associated number of cycles n_{wi}.

These loads are first extrapolated over the height of the structure to obtain the range of bending moment $\Delta M_{wind,i}$ at each node i (see equation 6).

$$\Delta M_{wind,i} = \Delta F_{x,top}.\Delta z_i + \Delta M_{y,top} \quad (6)$$

where $\Delta F_{x,top}$ = range of axial load at tower top; $\Delta M_{y,top}$ = range of bending moment at tower top; Δz_i = distance between the concerned structural detail and the top of wind tower.

The histogram of normal stress ranges $S_{wind,i}$ is then computed on the basis of the section characteristics (equation 7) and the Miner rule is finally applied to assess the cumulative fatigue damage $D_{Fat,wind}$.

$$S_{wind,i} = \frac{\Delta M_{wind,i}}{W_i} \quad (7)$$

where W_i = section modulus at the level of the structural detail i.

4.5 *Ultimate limit states*

4.5.1 *Design loads*

The ultimate limit state analysis implemented in this early optimization design stage considers six distributions of internal loads which are:

- F_x: shear force in x-direction;
- F_y: shear force in y-direction;
- F_z: vertical force;
- M_y: bending moment in Oxz-plane;
- M_x: bending moment in Oyz-plane;
- M_z: torque in z-direction.

For each load case considered in the design procedure, those distributions of internal loads result from the superposition of the three following actions:

1. Action of wind on the rotor and nacelle;
2. Action of wind pressure over the height of the emerged tubular structure;
3. Action of waves on the substructure.

The 3D configuration of these three actions is presented on Figure 8.

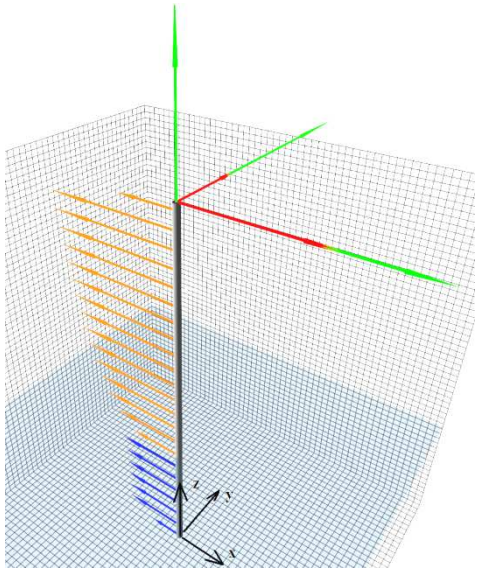

Figure 8. Distribution of wind and waves actions considered for the ultimate limit state analysis.

Similarly to the procedure developed for the assessment of fatigue strength, wind loads on the rotor and nacelle are first replaced by a set of equivalent punctual loads multiplied by safety coefficients and directly applied at the top of the offshore wind turbine.

Secondly, a pseudo-elastic calculation is performed to assess wind loading on the tubular structure. A power law profile is chosen for the distribution of wind speed v_{wind} and the corresponding wind pressures $q_{Sd,wind}$ are evaluated according to equation 8.

$$q_{Sd,wind}(z) = \frac{1}{2}\rho_a.C_{wind\ press}.v_{wind}(z)^2 \quad (8)$$

where ρ_a = air density; $C_{wind\ press}$ = safety coefficient on wind pressures; v_{wind}: wind speed given by the power law distribution; z = vertical position.

The resulting drag load $W_{Sd,wind\ drag}$ per meter applied at height z is found from expression 9.

$$W_{Sd,wind\ drag}(z) = c_d(z).q_{Sd,wind}(z).D(z) \quad (9)$$

where c_d = drag coefficient calculated from specifications prescribed by [5]; D = diameter of the tubular structure at height z.

This drag load is to be multiplied by a gust response factor G to account for the dynamic amplification of the structure response (equation 10).

$$W_{Sd,wind\ press}(z) = G\ W_{Sd,wind\ drag}(z) \quad (10)$$

where $W_{Sd,wind\ press}$ = design load due to wind pressure on the tower.

In the third part, the computation of internal loads due to waves is performed through a dynamic analysis of the support structure in the time domain.

The water elevation characterizing a load case is taken into account and a regular wave profile is gen-

erated from the wave height H_{wave} and period T_{wave} introduced in the environmental data.

The values for horizontal velocity v_w and acceleration a_w of water particles at each time step are then derived from the linear wave theory (Airy) corrected with the Wheeler stretching formulation in order to describe their kinematics in terms of instantaneous surface elevation (see equations 11 and 12).

$$v_w(z,t) = \frac{1}{2} H_{wave} \left(\frac{2\pi}{T_{wave}}\right) \frac{\cosh\left(k_{wave} \cdot \frac{d.z^*}{d+\xi(t)}\right)}{\sinh(k_{wave} d)} cos\left(-\frac{2\pi}{T_{wave}} t\right) \quad (11)$$

$$a_w(z,t) = \frac{1}{2} H_{wave} \left(\frac{2\pi}{T_{wave}}\right)^2 \frac{\cosh\left(k_{wave} \frac{d.z^*}{d+\xi(t)}\right)}{\sinh(k_{wave} d)} sin\left(-\frac{2\pi}{T_{wave}} t\right) \quad (12)$$

where H_{wave} = wave amplitude; T_{wave} = wave period; k_{wave} = wave number; d = water depth including water elevation; z* = z-position from sea bed level; ξ = instantaneous surface elevation; t = time.

The water particle kinematic is used to assess the hydrodynamic drag (equation 13) and inertia loads (equation 14) that are finally summed together to assess each component $F_{wave,i}(t)$ of the load vector $[F_{wave}]$ at time t.

$$F_{i,wave\ drag}(t) = \frac{1}{2} . \rho_w . C_d . D_i . L_i . |v_w(z_i,t)| . v_w(z_i,t) \quad (13)$$

$$F_{i,wave\ inertia}(t) = \rho_w . C_m . \pi . \frac{D_i^2}{4} . L_i . a_w(z_i,t) \quad (14)$$

where ρ_w = water density; C_d = hydrodynamic drag coefficient; C_m = hydrodynamic inertia coefficient; D_i = outer diameter of the monopile at node i; L_i = exposed height at node i; z_i: height of the node i.

The displacements vector $\vec{x}$ of the structure at the time step t result from the superposition of the eigen modes weighted by their respective dynamic amplification factors q_k (equation 15). Dynamic amplification factors are assessed iteratively on the basis of the structure and load vector thanks to the Newmark method.

$$\overrightarrow{x(t)} = \sum_{k=1}^{n_{ddl}} q_k(t) . \overrightarrow{V_k} \quad (15)$$

where $q_k(t)$: dynamic amplification factor of the mode k; $\overrightarrow{V_k}$: k^{th} eigen vector of the structure.

The displacement vector is then used to assess the evolution of internal loads of the support structure submitted to waves actions and the maximum values observed over the simulation are listed.

The distributions of internal loads obtained for each load case are finally combined to find the envelop diagrams of the support structure.

4.5.2 *Structural check*

The strength of each shell ring submitted to the design loads defined in the previous paragraph is checked according to the specifications given in DNV [4] or Germanischer Lloyd rules [3]. The following failures modes are considered:

- Shell buckling of unstiffened shell rings;
- Panel stiffener buckling of longitudinally stiffened shell rings;
- Panel ring buckling of transversally stiffened shell rings;
- Overall buckling of orthogonally stiffened shell rings.

An additional constraint is also implemented for the overall buckling of the column.

5 DESCRIPTION OF THE OPTIMIZATION PROCESS

5.1 *Design variables*

The design variables selected for the optimization process are divided in two categories:

- Shell ring variables: shell thickness, lower and upper diameters of the ring, steel grade;
- Segment variables: number and profile of longitudinal and ring stiffeners distributed respectively over the circumference and the height of the segment.

The height of shell rings and segments are not supposed to change during the optimization as they are considered as geometrical data fixed by the designer and the manufacturer of the structure.

5.2 *Description of the optimizer algorithm*

The algorithm chosen for the problem presented in this paper is a genetic algorithm (GA). Genetic algorithms are search algorithms that work via the process of natural selection. They begin with a sample set of potential solutions which evolves towards a set of more optimal solutions after several iterations. Within the sample set, poor solutions tend to die out while better solutions mate and propagate their advantageous traits, introducing better solutions into the set (though the total set size remains constant). A little random mutation guarantees that a set won't stagnate while filling up with numerous copies of the same solution.

In general, genetic algorithms tend to work better than traditional optimization algorithms because they are less likely to be led astray by local optima. This is because they don't make use of single-point transition rules to move from one single instance to another in the solutions space. Instead, GA's take advantage of an entire set of solutions spread throughout the solution space, all of which are experimenting upon many potential optima.

However, a few criteria must be met in order for GA to work effectively:

- The assessment of “how good” a potential solution is compared to other potential solutions must be relatively easy;
- The breaking of a potential solution into independent discrete parts must be possible;
- Genetic algorithms are best suited for situations where a "good" answer will suffice, even if it is not the absolute best answer.

5.3 *Evaluation of potential solutions*

The "fitness function" is responsible for performing the evaluation of solutions compared to each other. Basically, this module returns a positive integer number, or "fitness value", that reflects how optimal the solution is: the higher the number, the better the solution.

The fitness values are then used in a process of natural selection to choose the potential solutions that will survive in the next generation and those that will die out. However it should be noted that natural selection process does not merely select the top x number of solutions. Instead, solutions are chosen statistically so that it is more likely for a solution with a higher fitness value to be selected, but it is not guaranteed. This tends to correspond to the natural world.

In the methodology developed in this study, the equation implemented to assess the fitness value combines the criteria of weight/cost minimization and the criteria related to the constraints (equation 16). The relative importance of each term is set thanks to a weighing coefficient f_P.

$$Fit_k = \alpha.\theta_k - \beta.\sum_{j=1}^{n_c}\frac{P_{j,k}}{n_c} \qquad (16)$$

where Fit_k = fitness value of the solution k; θ_k = criterion of objective function minimization given by the ratio between the minimum value of the objective function and the value of the objective function for solution k; $P_{j,k}$ = penalty associated to the constraint j for the solution k (see equation 17); n_c = number of constraints; $\alpha = f_P$; $\beta = 1/f_P$; f_P = weighing coefficient.

$$P_{j,k} = \begin{cases} 0 & \text{if the constraint j is satisfied} \\ 1 - \left(\frac{C_{max,j,k}}{C_{j,k}}\right) & \text{if not} \end{cases} \qquad (17)$$

where $C_{max,j,k}$ = maximum permissible value for the constraint j in the solution k (for example the maximum permissible stress to avoid shell buckling of unstiffened panels) and $C_{j,k}$ = value found for constraint j in the solution k (for example the design Von Mises stress computed in the ultimate limit states analysis of the solution k).

The goal of the optimizer is to increase the fitness: this is done while decreasing the weight (or the cost) and satisfying as much structural constraints as possible.

6 OPTIMIZATION OF A 5MW OFFSHORE WIND TURBINE

6.1 *Generals*

The computerized tool has been tested on the scantling of a 5MW offshore wind turbine. The characteristics of the support structure, environmental conditions, optimisation parameters and results are described hereafter.

6.2 *Characteristics of the offshore wind turbine*

The main characteristics of the wind turbine are summarized in the Table 1 below.

Table 1. Characteristics of the 5MW offshore wind turbine

Description	Value	Unit
Wind turbine power	5	[MW]
Number of blades	3	[-]
Rotor diameter	118	[m]
Nacelle mass (incl. rotor blades)	390	[tons]
Speed range	4 – 14.2	[min^{-1}]

The initial monopile support structure considered in the study is made of steel S235 and its general dimensions are listed in Table 2.

Table 2. Characteristics of the initial monopile support structure (steel grade S235)

Description	Value	Unit
Hub height (above MSL)	80	[m]
Tower length (above MSL)	77	[m]
Length between MSL and seaground	30	[m]
Height of shell ring below seaground	5	[m]
Outer shell diameter at top	4	[m]
Outer shell diameter at seaground	5.7	[m]
Shell thickness at top	25	[mm]
Shell thickness at seaground	115	[mm]
Weight	902.1	[tons]

Concerning the dynamic of the structure, the logarithmic decrements on the first mode due to structural and aerodynamical damping were assumed equal to 0.012 and 0.01 respectively.

6.3 *Environmental conditions*

6.3.1 *Data related to fatigue analysis*

The scatter diagram taken into account to assess wave induced fatigue is made of 15 typical sea states observed in the North Sea [1].

Fluctuating wind loads were calculated by an external bureau of study for the wind turbine placed in a dynamic pressure zone IEC IA (see Table 3).

Table 3. Wind parameters for dynamic pressure zone IEC IA

Description	Value	Unit
Reference wind speed V_{ref}	37.5	[m/s]
Average wind speed V_{ave}	10	[m/s]
Intensity of turbulences I	0.18	[-]

The cumulative fatigue damages due to wind and wave action for each butt weld of the structure are listed in the table 4 below. Note that the category of detail for butt welds is set to 112.

Table 4. Values of cumulative fatigue damages for the initial scantling S235

Section	z-position [m]	$D_{fat,wave}$ [-]	$D_{fat,wind}$ [-]	D_{fat} [-]
23	110 (tower top)	9.154e-9	8.425e-4	8.425e-4
22	105	1.077e-5	0.007	0.007
21	100	1.235e-4	0.023	0.023
20	95	3.534e-4	0.030	0.030
19	90	7.260e-4	0.040	0.041
18	85	0.002	0.068	0.070
17	80	0.003	0.083	0.086
16	75	0.004	0.085	0.089
15	70	0.005	0.101	0.106
14	65	0.006	0.106	0.112
13	60	0.009	0.124	0.133
12	55	0.009	0.117	0.126
11	50	0.012	0.138	0.150
10	45	0.014	0.139	0.153
9	40	0.017	0.150	0.167
8	35 (MSL)	0.019	0.161	0.180
7	30	0.020	0.156	0.176
6	25	0.021	0.152	0.173
5	20	0.019	0.130	0.149
4	15	0.014	0.091	0.105
3	10	0.012	0.082	0.094
2	5 (seaground)	0.012	0.070	0.082
1	0 (clamping)	0.012	0.070	0.082

6.3.2 *Data related to ultimate limit states*

Time domain simulations were performed by the bureau of study with the software NREL aerodyn to establish the set of extreme tower top loads due to the wind action coupled with the rotor dynamics. These data are not presented in this paper for confidentiality reasons.

The distribution of extreme wind speeds over the tower height is based on the power law coefficient with an exponent α equal to 0.14 and the highest occurring wind speed V_{e50} at hub height for a recurrence period of 50 years (equation 18).

$$V_{e50} = 1.25\, V_{ref} = 62{,}5\ m/s \qquad (18)$$

The extreme wave profile considered in the optimization process is a regular wave profile characterized by a wave height H_w and wave period T_w equal to 10m and 14s respectively. No current or water elevation compared to MSL were assumed in this load case.

Figure 9 shows the envelop diagrams of internal loads generated by the software for the initial scantling S235 placed in the environment described previously.

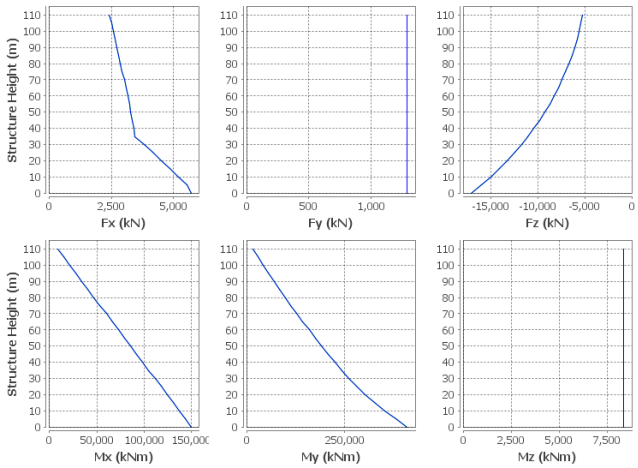

Figure 9 – Envelop diagrams of internal loads for the initial scantling S235

6.4 *Optimization parameters*

The optimization carried out was based on the minimization of the structural weight of the offshore wind structure.

As the methodology aims to highlight the advantages of using high tensile steel in offshore structures, this optimization was performed on an unstiffened structure made of conventional steel grade S355.

The design variables selected for the process were the shell thickness (ranging from 8 to 150mm), lower and upper diameters of shell rings (ranging from 4 to 6m). Optimizations based on the variation of number and profiles of stiffeners were not envisaged.

6.5 *Optimization results*

The evolution of the structural weight and production cost during the optimization process for the unstiffened structure made of steel S355 is presented on Figure 10. It can be seen that the convergence to the optimum solution is ensured after about 1000 iterations.

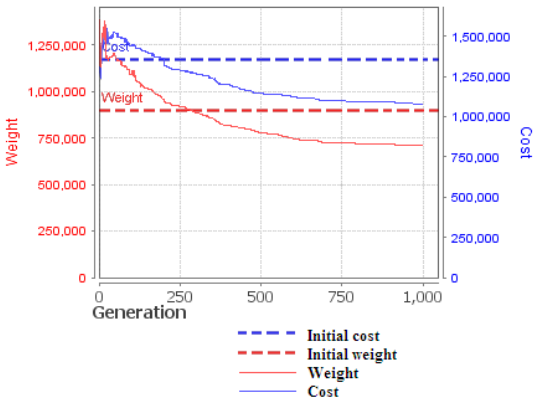

Figure 10 - Evolution of weight and production cost during the optimization process of the structure S355

The general characteristics of the optimum solutions made of steel S355 are summarized in the table 4 presented below.

Table 4. General characteristics of optimal scantlings S355

Description	Value	Unit
Diameter at top	4	[m]
Diameter at seaground	5.3	[m]
Shell thickness at top	22	[mm]
Shell thickness at seaground	94	[mm]
Structural Weight	712.5	[tons]

In this optimum scantling, the values of shell rings diameters are slightly lower than in the initial scantling but only for the lower part of the structure (see Figure 11).

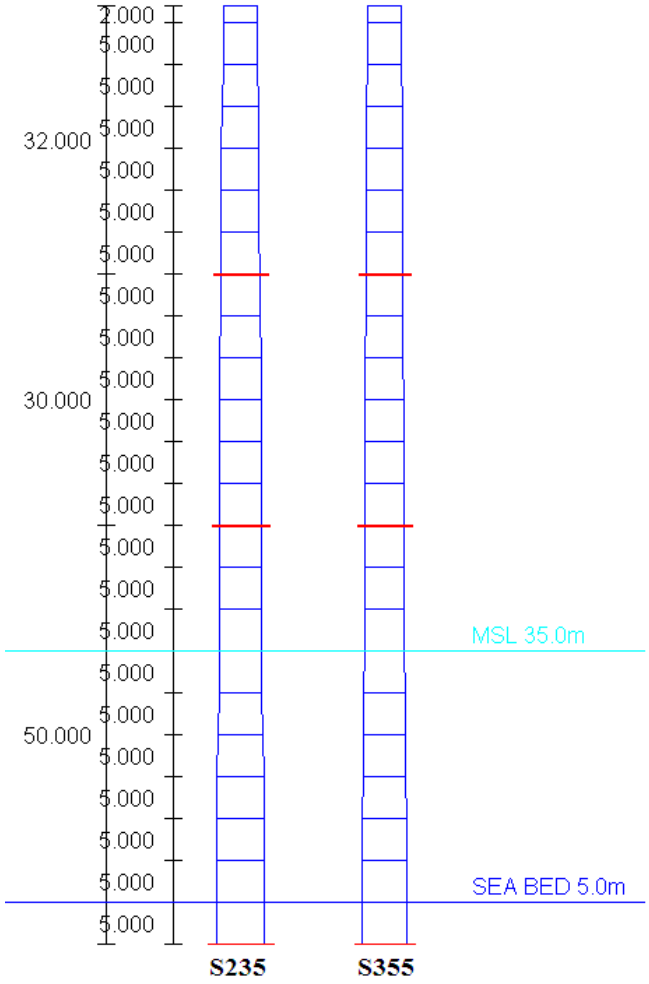

Figure 11 - Drawings of initial scantling S235 and optimal scantlings S355

On the other hand, the shell thicknesses are significantly lower in the optimal solution S355. This leads to weight and cost reductions equal to 21% and 20.4% respectively compared to the initial scantling made of steel S235.

7 CONCLUSION

In this paper, an optimization tool dedicated to the early design stage of steel monopile offshore wind turbines has been described. Constraints related to the structural integrity of the support structure are assessed and an optimum solution in terms of weight or production cost is obtained thanks to a genetic algorithm.

The dimensions of the support structure are reduced while using high tensile steel instead of normal steel grade. As an example, the optimization tool showed that the saves in terms of weight and production cost can reach about 20% when steel grade S235 is replaced by steel S355.

Finally, a certain number of elements could be added to the methodology in future developments. First, the optimization process could be extended to the scantling of the underground part of the support structure. Second, if the coupling between fluctuating wind loading and structure dynamic is considered at each step of the iteration process, the accuracy of the cumulative damage found from the fatigue analysis would be improved. And finally, some phenomena such as irregular wave profiles, marine currents, ice and marine growth formation could be taken into account in ultimate limit state analyses.

8 REFERENCES

[1] VAN DER TEMPEL, J. 2006. *Design of Support Structures for Offshore Wind Turbines*, PhD Thesis, Delft University of Technology, ISBN 90-76468-11-7

[2] KÜHN, M. 2001. *Dynamics and Design Optimisation of Offshore Wind Energy Conversion System*, PHD Thesis, Delft University of Technology, Section Wind Energy, Department of Civil Engineering

[3] *Guideline for the Certification of Offshore Wind Turbines*, Germanischer Lloyd WindEnergie, edition 2005

[4] *Recommended Practice DNV-RP-C202 – Buckling Strength of Shells*, Det Norsk Veritas, October 2002

[5] *Eurocode 1: Bases de calcul et actions sur les structures*, May 1995

[6] KÜHN M., COCKERILL T.T., HARLAND L.A., HARRISON R., SCHÖNTAG C., VAN BUSSEL G.J.W., VUGTS J.H. 1998. *Opti-OWECS Final Report Vol.2: Methods Assisting the Design of Offshore Wind Energy Conversion Systems*, Delft University of Technology, ISBN 90-76468-03-6